Indirect Susceptibility Mapping of Thin-Layer Samples Using Nuclear Magnetic Resonance Imaging

Ivan Frollo, Peter Andris, Jiří Přibil, and Vladimír Juráš

Institute of Measurement Science, Slovak Academy of Sciences, Bratislava 84104, Slovakia

We measured and imaged magnetic field distributions of thin layers (2-D objects with negligible thickness) of biological and physical samples, by using nuclear magnetic resonance (NMR). The image represents the magnetic susceptibility distribution in the sample. We used a standard gradient echo imaging method, susceptible to magnetic field homogeneity, for detection. Since the physical and biological samples we investigated do not generate any NMR signal, we used a homogeneous phantom reference—a container filled with water—as a medium. The image acquired by this method is actually a projection of the sample properties onto the homogeneous phantom. The method can be applied in nanotechnology, microelectronics, and especially in the biological and medical sciences.

***Index Terms*—Magnetic liquids, magnetic resonance imaging, magnetic susceptibility, thin layers.**

I. Introduction

IMAGING of ferromagnetic or paramagnetic objects that do not incorporate any water molecules and do not generate any nuclear magnetic resonance (NMR) signal is not possible by using standard MRI methods. Inserting such objects into a stationary homogeneous magnetic field results in field deformation proportional to the susceptibility of the sample. If the space in the vicinity of the sample is filled with a water containing substance, we are able to image this sample. In the case of a homogeneous phantom (e.g. a slender rectangular container filled with water), the acquired image represents a modulation of the local magnetic field, displaying the magnetic susceptibility distribution in the sample.

By using an appropriate mathematical model it is possible to calculate this susceptibility, but in a real sample the susceptibility is imperfectly uniform along the three spatial axes, making any inversion approach model-dependent and nonexact. Assumptions underlying the theoretical development are not clear, especially regarding the shape of the sample.

The first attempt of a direct measurement of the magnetic field created in living tissue by a simple wire fed by a current was reported in [1]. The report described an experiment in which magnetic fields produced by a small current applied to the forearm of a living subject have been detected in the tissue. Initial experiments were performed *in vitro*, using a cylindrical phantom. A current was passed along the inner of two concentric cylinders filled with conductive saline and a spin-echo NMR imaging sequence was used for signal detection. The phase-image computed from the real and imaginary images demonstrated the presence of a magnetic field in the cylinder.

A method utilizing the divergence in gradient strength that occurs in the vicinity of a thin current-carrying copper wire was introduced in [2]. Using pulsed gradient spin-echo NMR sequence, *in vitro* micro images of a sample, a solution of polyethylene oxide in water, were presented. The paper showed the effect of molecular diffusion in the vicinity of a thin wire subjected to current pulses. This effect was performed in measurements on polymer solutions and liquid crystals.

A simple experiment with thin, pulsed electrical current-carrying wire and imaging of a magnetic field using a plastic sphere filled with agarose gel as phantom, was published in [3]. Images of the phantom were obtained with and without application of electric current to a straight wire using a spin-echo NMR sequence. Because the method proposed in the study did not use phase images, phase unwrapping was not required. The method is designed for the detection of electric currents in biological tissues by observations of surface potentials or surrounding magnetic fields.

NMR imaging is an effective method for indirect mapping of magnetic field distributions. Based on NMR principles, we propose a new 2-D method for indirect susceptibility mapping and imaging of ferromagnetic or paramagnetic samples placed into the homogenous magnetic field of an NMR scanner. For testing and calibration of the method a double flat coil—a meander, fed by electric currents and generating a weak magnetic field, was used.

Our task was to map the magnetic field deformation (MFD) and to image the specific structure of the thin 2-D ferromagnetic or paramagnetic samples using NMR imaging methods. In our experiments, we use a slender rectangular vessel with constant thickness filled with specially prepared water (*vide infra*). A carefully tailored gradient echo (GE) NMR measuring sequence was used.

II. Purposes and Method

A. Magnetic Field Deformation Theory

Suppose we have an ideally homogeneous magnetic field generated by an air-core electromagnet. When a ferromagnetic or paramagnetic object is placed into this homogeneous magnetic field, the magnetic induction is as follows:

$$B = \mu H = \mu_0 \mu_r H = \mu_0 H + J \tag{1}$$

where

$\mu_r = \mu / \mu_0$	relative permeability;
J	intensity of magnetization.

Digital Object Identifier 10.1109/TMAG.2007.900571

Color versions of one or more of the figures in this paper are available online at http://ieeexplore.ieee.org.

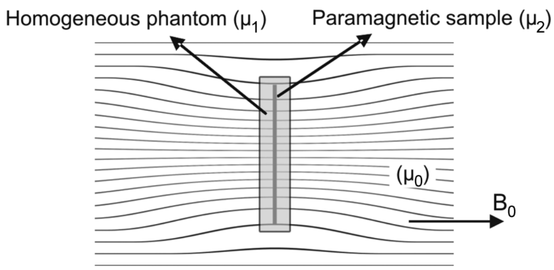

Fig. 1. Planar paramagnetic sample inserted into the homogeneous magnetic field causes deformation of magnetic field lines. The sample is immersed into the holder with water (homogeneous phantom).

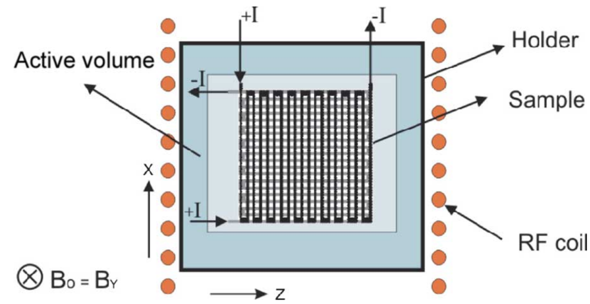

Fig. 2. Orientation of the RF coil, active measuring volume (holder—phantom) and sample (double flat coil) in the magnetic resonance imager.

From (1), we can write for intensity of magnetization

$$J = \mu_0\mu_r H - \mu_0 H = \mu_0(\mu_r - 1)H = \chi H \quad (2)$$

where $\chi = \mu_0(\mu_r - 1)$ is an absolute susceptibility of the ferromagnetic object [4].

In general, placing a thin ferromagnetic or paramagnetic sample with $\mu_r = \mathrm{const.}$ into the homogeneous magnetic field, the MFD appears in the objects and in the surrounding space near the object (see Fig. 1).

For simplicity, the MFD can be expressed as a deflection of the magnetic field lines (φ_1, φ_2) on the border of two isotropic media (μ_1, μ_2).

For magnetic field lines, deflection in two isotropic magnetic boundaries follows:

$$tg\varphi_1/tg\varphi_2 = \mu_1/\mu_2 = \mu_{r1}/\mu_{r2}. \quad (3)$$

The aim of this paper is to detect and to image the magnetic field deformation values for selected samples.

B. Experimental Configuration

In our experiment, two MR imagers with different field strengths were used (0.1 and 4.7 T). The sample was placed in a plastic bushing and inserted into a vertical, rectangular holder (phantom) filled with 0.1 wt% solution of $CuSO_4$ in distilled water. $CuSO_4$ was used to shorten the repetition time TR to 200 ms due to its reduction of H_2O T_1 (for speeding up of the data collection). The basic configuration of our experiment is shown in Fig. 2. In our experiments we used a holder filled with doped water (inner dimensions 60 × 60 mm, constant inner thickness 10 mm). Any sample inserted into the holder changes its inner water thickness, however.

An RF transducing coil together with the sample and phantom were placed in the center of the electromagnet, perpendicular to the magnetic field (B_0) orientation. A solenoid detection coil was designed with the goal to optimize the RF field homogeneity (Fig. 3).

C. Modeling and Testing

For testing and calibration of the method a double flat coil—meander—produced on a printed board, with a thickness of 0.5 mm (see Fig. 2) was selected. Feeding currents $+\mathrm{I}$ and $-\mathrm{I}$ were selected to create a planar source of a weak magnetic field in the shape of a grid. Each individual conductor had a length $2L$. The conductor's position on the z-axis was given by a and the separation of the front and rear layers (turned over 90°) was $2b$. The magnetic field of the front layer generated by such a system is easy to calculate using the Biot–Savart law [5]. The resulting formula describing the field is in the form

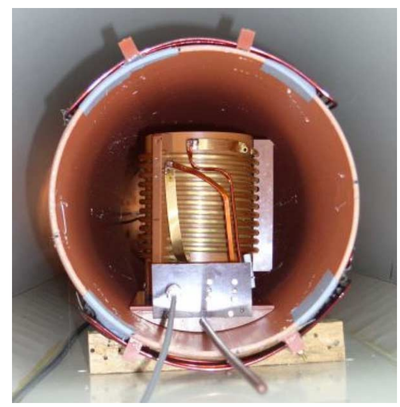

Fig. 3. RF coil located in the magnetic field of a magnetic resonance imager. A cylinder around RF coil represents a gradient coil system designed specially for this experiment.

$$H_y(x,y,z) = \frac{I}{\pi}\sum_{n=1}^{10}\sum_{i=1}^{2} W_{in}V_{in} \quad (4)$$

where

$$V_{in} = \frac{b_i - y}{(a_n - z)^2 + (b_i - y)^2}$$
$$W_{in} = \mathrm{Sin}\left[\mathrm{ArcTan}\left(\frac{L-x}{a_n - z}\right)\right] + \mathrm{Sin}\left[\mathrm{ArcTan}\left(\frac{L+x}{a_n - z}\right)\right]$$

n	index determinating a numerical order of a wire in a quadrant, first wires of the left and right quadrants are interlaced;
a_n	position of a conductor on the z-axis for $\mathrm{n} = 1$ to 10;
b_i	half distance of layers of conductors;
i	number of layers of conductors;
L	half length of each individual conductor.

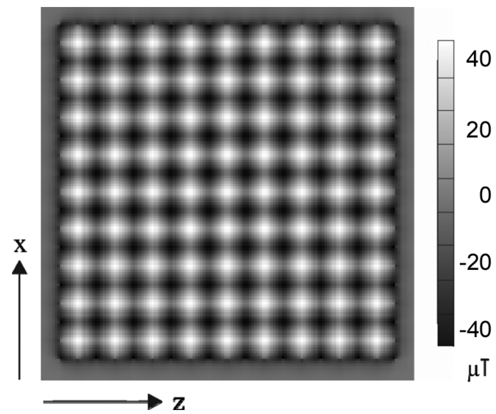

Fig. 4. Density plot of magnetic field for $y = 0$ for coil layer (meander): 50 × 50 mm, 19 wires in each layer, distance of layers of conductors $\mathrm{b} = 1$ mm.

By reciprocally exchanging the variables x and z we obtain an adequate expression for the rear layer. The resultant magnetic field is a sum of two expressions, one for the front plane $(\mathrm{b_i} = \mathrm{b})$, one for the rear plane $(\mathrm{b_i} = -\mathrm{b})$. The currents of the front and rear planes are oriented in opposite directions; $+\mathrm{I}$ and $-\mathrm{I}$.

Fig. 4 shows the density plot of the magnetic field for $y = 0$ (the middle plane between the front- and rear-layers), using 150 points. The dimensions of the coil layer (meander) were: 50 × 50 mm, 19 wires in each layer symmetrical with respect to the central axis.

D. Imaging Sequence

The "Gradient Echo" NMR sequence (Fig. 5) was selected for the measurement [5]. A special feature of the sequence is its sensitivity to basic magnetic field inhomogeneities.

A 5-lobe sinc pulse selectively excited the sample. The dimensions of the vessel with the sample determined the slice thickness, therefore the slice gradient was switched off. Images were obtained with a field of view of 120 mm. The number of samples and the number of views determining the final resolution were 128 each and the echo time TE was 32 ms. To increase the signal-to-noise ratio of the data, the signals were averaged 16 times. For MFD representation a phase image was calculated using the phase unwrapping method [9].

In the first step—for method calibration and testing—various feeding currents were connected to the meander coil. The maximum current was limited by the amplitude of the NMR output-signal which decreased (by influence of increasing inhomogeneities) with the increase of feeding current. For our experiment, a current of 30 mA showed to be a good compromise. The first results of MFD imaging of the meander flat coil are depicted in Fig. 6. The actual image of this sample has 64 × 64 pixels.

There is a good correspondence of images comparing the computed image in Fig. 4 with an image gained by NMR method, Fig. 6. As to the quantitative agreement, the NMR image (in comparison with the basic magnetic field of the scanner 0.1 T) represents MFD of the meander coil in the range of 0 to 89.75 μT. The small differences between calculated and measured values are determined by nonlinearities of the r.f. coil and local inhomogeneities of the basic magnetic field.

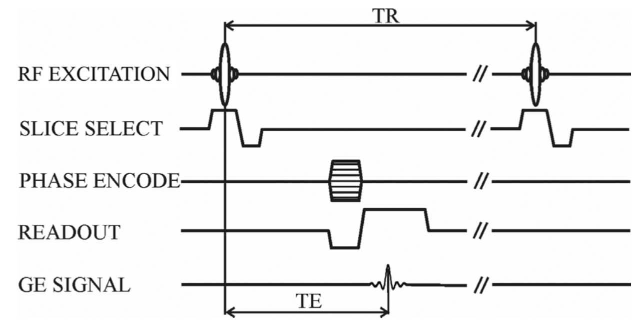

Fig. 5. Time diagram of the NMR sequence for the gradient echo signal detection. TE—echo time 32 ms, TR—repetition time 200 ms.

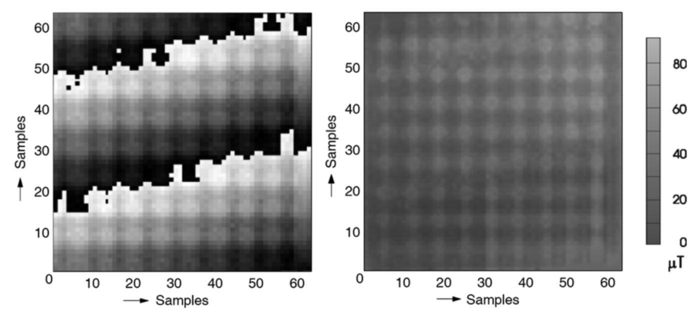

Fig. 6. Image of the MFD of a meander flat coil (50 × 50 mm), number of measured samples 128 × 128, 0.1 Tesla MR Imager. Actual image of this specimen was associated with 64 × 64 pixels. Left: phase image calculated from the measured data. Right: image representing MFD calculated from phase data after application of phase unwrapping method.

The model (double meander coil) served for the verification of the methodology, for the adjustment of basic parameters of the imaging sequence: time intervals TE and TR, number of averages, and for the testing of a reference environment—$CuSO_4$ doped water related to relaxation times of measuring sequence.

E. Using Magnetic Liquids

Magnetic liquids (ferrofluids) are stable colloidal suspensions composed of single-domain magnetic nanoparticles dispersed in appropriate solvents [6], [7]. In general, magnetic particles are derived from the solid solution of the spinel $\mathrm{Mn_xFe_1 - xFe_2O_4}$. Surfactants are added during the synthesis of magnetic liquids to surround the small particles and overcome their attractive tendencies [10].

In the absence of a magnetic field each particle may be considered independent and its magnetization direction is randomly oriented, hence such a system resembles a paramagnetic gas. However, when the number density or magnetic moment of the magnetic particles is large, one cannot neglect dipole–dipole interactions between particles. Such interactions may be manifested in the dynamical magnetic properties of magnetic liquids.

In this work, magnetite $(\mathrm{Fe_3O_4})$ particles were prepared by chemical precipitation of $FeCl_2$ and $FeCl_3$ (1:2 molar ratio) by the addition of 25% ammonia solution. In a typical reaction (5): 2.1 g $FeCl_2$ and 5.9 g $FeCl_3$ were mixed in 100 ml water and heated to 80 °C [8].

$$2\mathrm{FeCl_3} + \mathrm{FeCl_2} + 8\mathrm{NH_3} + 4\mathrm{H_2O} \rightarrow \mathrm{Fe_3O_4} + 8\mathrm{NH_4Cl}. \quad (5)$$

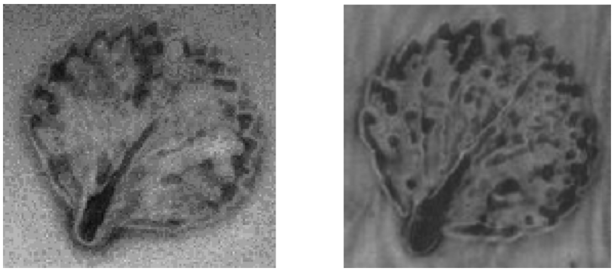

Fig. 7. Sample dimension: leaf $\Phi = 30$ mm. Left: sampling 256 × 256, resolution 230 μm, 0.1 T. Right: sampling 512 × 512, resolution 100 μm, 4.7 T.

In order to get an aqueous-based magnetic fluid, tetramethylammonium hydroxide, $(CH_3)_4N(OH)$, was used as a surfactant [11].

It is possible to use various methods to coat the samples with a magnetic substance: soaking in a diluted magnetic liquid, using an oriented spray, steaming with magnetic steam, sputtering of the pulverized form. The goal is to ensure homogeneous application of the magnetic substance onto the sample. During the soaking method, magnetic liquid can be absorbed in the sample which could cause some changes of biological and physical properties. Hence, it is important to distinguish living and desiccated samples (with a minimum of original liquid). For sample preparations in our experiments, water solution of the magnetic liquid was diluted by 1:500.

F. Imaging of Thin Layers

The first experiment on a biological sample was performed. A magnetic liquid with a dilution factor of 1:500 for a biological sample preparation was used. A dry leaf was immersed into such solution for 24 h. After drying, the samples were stuck on a sheet of paper and inserted into a protective plastic bushing. The bushing with the sample was squeezed to the water phantom. The best results were achieved when the bushing was immersed into water.

Using a gradient-echo, the slice selective gradient $\mathrm{G_y}$ was omitted. The $\mathrm{G_x}$ gradients ensured the phase encoding and the $\mathrm{G_z}$ gradients the readout of the NMR signals in the shape of the gradient echo.

The holder dimensions were 60 × 60 × 10 mm. The image resolution was 256 × 256 or 512 × 512 pixels and the number of averages was 16 (Fig. 7).

For the next experiment on a physical sample, the letters "NMR" with the dimension of 55 × 17 mm were printed, using a magnetic liquid on a sheet of standard business paper. The sample was positioned in a plastic holder and placed into the vertical rectangular container (phantom) filled with 0.1 wt% solution of $CuSO_4$ in distilled water. The image was sampled with 512 × 512 samples, the number of averages was 16, the resolution 150 μm, and the static magnetic field $\mathrm{B_0} = 0.1$ T (Fig. 8).

Because of the relatively high susceptibility of the printed letters, a corona appeared around the pattern. This phenomenon is caused by the fact that the water layer is high in comparison with the sample thickness. The detected magnetic field is actually an averaged projection of magnetic field lines. Reducing the thickness of the liquid in the phantom increases the sharpness and quality of the sample image. The corona would be reduced, but the signal-to-noise ratio would subsequently decrease.

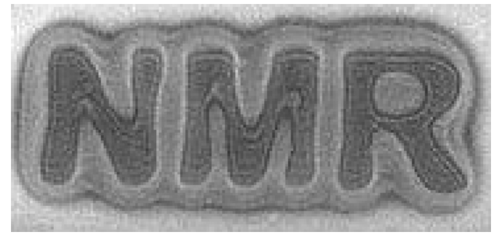

Fig. 8. Image of letters "NMR," dimension 55 × 17 mm, 512 × 512 samples.

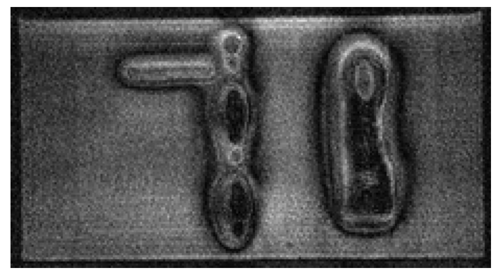

Fig. 9. Magnetic image of a banknote with visible "magnetic islands," 512 × 512 samples.

The next exciting experiment was performed on a physical sample, a banknote equipped with hidden integrated magnetic signs (for security reasons, the origin is not published). The banknote was positioned in a plastic holder and placed into the vertical rectangular container (water phantom). The image was sampled with 512 × 512 samples, the number of averages was 16, the resolution 150 μm, and the static magnetic field $\mathrm{B_0} = 0.1$ T (Fig. 9).

The experiment revealed the following facts:

It is evident that linear projection of the magnetic quantities of the sample into the phantom can be performed only when the vector of the static magnetic field $\mathrm{B_0} = \mathrm{B_y}$ is perpendicular to the sample plain. Other orientations caused significant blurring of the image edges in the y-axis direction due to strong basic magnetic field $\mathrm{B_0}$.

The reduction of the RF sensor and phantom vessel dimensions and use of a special gradient coil system with smaller dimensions will allow the acquisition of images with high resolution (micro imaging). NMR signal from a small RF sensor (high quality RF coil) close to the sample will have a higher signal-to-noise ratio.

Image correction, from the reason of inhomogeneities of the static magnetic field is possible by subtraction of the phase images of the phantom without a sample, and the phantom with a sample. Because of the relatively high susceptibility of the samples, the resultant image correction was not necessary.

III. Conclusion

A new method for an indirect susceptibility mapping and imaging of planar ferromagnetic or paramagnetic samples placed into the homogenous magnetic field of an NMR imager is proposed. The method is based on the projection of magnetic domains into a homogeneous planar phantom (slender vessel with specifically prepared water) and subsequent NMR imaging using a gradient-echo sequence.

The method was tested using a double flat coil—meander—fed by electric currents generating weak magnetic field.

Three examples documented the capability of the proposed method to map and image the magnetic susceptibility distribution on samples not containing any water. Experiments on a biological sample and on a printed picture, using a magnetic liquid and on a document comprising hidden integrated magnetic signs were performed.

The first results showed the feasibility of the method and some possibilities offered in this field of research.

Acknowledgment

This work was supported by the Grant Agency of the Slovak Academy of Sciences, project no. 2/5043/27 and Agency for Science and Technology Support, project no. APVV-99-P06305.

References

[1] M. Joy, G. Scott, and M. Henkelman, “In vivo imaging of applied electric currents by magnetic resonance imaging,” *Magn. Res. Imag.*, vol. 7, pp. 89–94, 1989.

[2] P. T. Callaghan and J. Stepisnik, “Spatially-distributed pulsed gradient spin echo NMR using single-wire proximity,” *Phys. Rev. Lett.*, vol. 75, no. 24, pp. 4532–4535, 1995.

[3] M. Sekino, T. Matsumoto, K. Yamaguchi, N. Iriguchi, and S. Ueno, “A method for NMR imaging of a magnetic field generated by electric current,” *IEEE Trans. Magn.*, vol. 40, no. 4, pp. 2188–2190, Jul. 2004.

[4] J. D. Kraus and D. A. Fleisch, *Electromagnetics With Applications*, 5th ed. New York: McGraw-Hill, 1998.

[5] Z.-P. Liang and P. C. Lauterbur, *Principles of Magnetic Resonance Imaging: A Signal Processing Perspective*. New York: Wiley-IEEE Press, 1999.

[6] R. V. Upadhyay, D. Srinivas, and R. V. Mehta, “Magnetic resonance in nanoscopic particles of a ferrofluid,” *J. Magn. Mater.*, pp. 105–111, 05/2000.

[7] M. I. Shliomis, A. F. Pshenichnikov, K. I. Morozov, and I. Y. Shurubor, “Magnetic properties of ferrocolloids,” *J. Magn. Magn. Mater.*, vol. 85, no. 1–3, pp. 40–46, 1990.

[8] M. R. Racuciu, D. E. Creanga, and G. Calugaru, “Synthesis and rheological properties of an aqueous ferrofluid,” *J. Optoelectron. Adv. Mater.*, vol. 7, no. 6, pp. 2859–2864, 2005.

[9] J. Přibil and I. Frollo, “A simple method of phase unwrapping for NMR images,” *J. Elect. Eng.*, vol. 57, no. 12/S, pp. 25–28, 2006, 1335-3632.

[10] D.-H. Kim, S.-H. Lee, K.-H. Im, K.-N. Kim, K.-M. Kim, K.-D. Kim, H. Park, I.-B. Shim, and Y.-K. Lee, “Biodistribution of Chitosan-based magnetite suspensions for targeted hyperthermia in ICR mice,” *IEEE Trans. Magn.*, vol. 41, no. 10, pp. 4158–4160, Oct. 2005.

[11] Z. G. M. Lacava, L. M. Lacava, M. J. P. Fonseca, T. M. M. Souza, L. O. Pereira, O. Silva, F. Pelegrini, D. Sabolovic, C. Sestier, R. Azevedo, N. Buske, and P. C. Morais, “Magnetic resonance and light microscopy investigation of raw cells treated with dextran-based magnetic fluid,” *IEEE Trans. Magn.*, vol. 42, no. 10, pp. 3599–3601, Oct. 2006.

Manuscript received November 14, 2006; revised May 14, 2007. Corresponding author: I. Frollo (e-mail: frollo@savba.sk).